Hierarchical Co_2P Microspheres Assembled from Nanorods Grown On Reduced Graphene Oxide as Anode Material for Lithium-ion Batteries

Chi Zhang [a,+], Guanghua Jiao [a,+] , Fanjun Kong [a], Jian Wang [a], Shi Tao [a,], Lei Zhang [a], Bin Qian [a,*], Yimin Chao [b]*

[a] *Department of Physics and Electronic Engineering, Jiangsu Laboratory of Advanced Functional Materials, Changshu Institute of Technology, Changshu 215500, China*

[b] *School of Chemistry, University of East Anglia, Norwich, NR47TJ, UK.*

[+] *The authors contributed equally to this work*

[*] *Corresponding author.*

E-mail: taoshi@cslg.edu.cn(S.Tao) ;njqb@cslg.edu.cn(B.Qian).

ABSTRACT

Transition metal phosphides (TMPs) have been studied as promising electrodes for energy storage and conversion due to their large theoretical capacities and high activities. Herein, a hierarchically structured Co_2P coupling with the reduced graphene oxide (RGO) composite (Co_2P/RGO) was synthesized by a simple solid state method for Li storage. The Co_2P/RGO hybrid composite exhibits a high reversible capacity of 610 mAh g^{-1} at 60 mA g^{-1}, good rate capability of 327 mAh g^{-1} at 3000 mA g^{-1} and long cycle life (397 mAh g^{-1} at 500 mA g^{-1} for after 1000 cycles). The excellent

electrochemical performance can be attributed to the synergistic effect of Co_2P micro/nano architecture and graphene modulation, which provide more activity sites for Li^+-ions and maintain the structural integrity of active material. This work may provide a new path for preparation of other metal phosphides as potential electrode materials for application in energy storage fields.

Keywords: Cobalt phosphide, Graphene, Hierarchical structure, Anode, Lithium-ion batteries

1. Introduction

With the increasing demand for renewable and sustainable energy sources, it is critical for developing advanced energy storage devices [1]. Among various energy storage devices, lithium-ion batteries (LIBs) have been widely used in application of electrical vehicles (EVs) and energy-storage systems (EESs), due to their high energy density, long lifespan and good rate performance [2,3]. Graphite is commonly used as commercial anode material, however, its limit theoretical capacity (372 mAh g^{-1}) and safety issues restrict its further application [4,5]. Therefore, it is an urgent task to serach novel anode materials for next-generation LIBs. To date, various alternative anode materials have been investigated including transition metal oxides (Fe_2O_3 [6,7], NiO [8], Co_3O_4 [9], SnO_2 [10,11]), sulfides (CoS_2 [12,13], FeS_2 [14,15], SnS_2 [16,17], MoS_2 [18,19]) and phosphides (NiP_2 [20], CuP_2 [21], FeP [22], Co_xP [23,24], Sn_3P_4 [25])

due to their remarkable theoretical capacities, low cost and natural abundance. Among these novel anode materials, transition metal phosphides (TMPs) demonstrate relatively low charge-discharge potentials, good thermal stabilities, and metallic features [26-28].

In particular, Co_2P has received increased attention due to its specific crystal configuration, which exhibits good stability inserted by Li^+-ions and exhibits high redox reacivity and high capacity for LIBs [29-32]. However, its intrinsically low electronic conductivity and large volume expansion during the charging-discharging process result in poor rate capability and cyclability. The combination of functional carbon materials (e.g., carbon tubes and graphene) has been proven an effectively way to enhance the electrochemical performance [33-35]. In addition, most of the existing methods to prepare Co_2P composites use the toxic alkylphosphine, organic reagent and surfactants, which limit its practical application. Thus, a simple synthetic process for TMPs involve the use non-toxic and inexpensive raw materials is highly expected.

In this paper, we present a simple solid-state strategy to synthesize hierarchical Co_2P microspheres/reduced graphene oxide (RGO) composite, which consists of interconnected nanorods grown on the RGO layers. The electrochemical results confirm that the performance of Co_2P was greatly enhanced by the RGO modification. Benefitting from the RGO wrapping and the micro/nano architecture, which can release the volume change and maintain the structural stability, the Co_2P/RGO hybrid composite delivers superior lithium storage properties.

2. Experimental section

2.1 Synthesis

Graphene oxide (GO) was synthesized by a modified Hummers method as the previous report [36]. For synthesis of Co_2P/RGO, 10 mg GO was dispersed in 30 mL distilled water and ultrasonic treatment for 1 h t. After that, 1 mmol $Co(CH_3COO)_2 \cdot 4H_2O$ were added into the above solution, then continuous stirring for another 2 h. The solution was transfer to air dry oven to evaporate water. The obtained powder was mixed 5 mmol NaH_2PO_2 and thoroughly ground to homogenous mixture in an agate mortar. The mixture was transferred to a porcelain boat, which was then wrapped with a piece of tinfoil paper. The half-sealed porcelain boat was put into a quartz tube, and then heated to 100 °C with a speed 5 °C/min under Ar atmosphere, maintaining at 100 °C for 30 min and then heated to 350 °C for 2 h. The obtained black powder was washed with distilled water and ethyl alcohol several times and dried in vacuum at 60 ℃ for 24 h. The bare Co_2P was prepared by direct mixing $Co(CH_3COO)_2 \cdot 4H_2O$ and Na_2HPO_2 and then was calcined at the same steps without using GO. The Co_2P-RGO mixture sample was synthesized by the simple direct ball mixing of Co_2P and RGO with a weight ratio of 10:1.

Materials characterization

The phase of as-prepared samples were tested by X-ray diffractometer (Bruker APEX) (Cu-K, λ=1.5406 Å). Scanning electron microscopy (FE-SEM, ZEISS) and transmission electron microscopy (TEM, JEOL- 2000CX) were applied to evaluated the morphology of samples. The thermogravimetric analysis (TGA, SDTA851) was used to estimate the graphene content in air. The X-ray photoelectron spectroscopy (XPS, ESCALAB 250) were employed to investigate chemical structure. Raman spectra were performed on Raman spectrometer (Horiba Xplora). The N_2 adsorption/desorption measurements were tested by an ASAP2020 instrument. The XANES (X-ray Absorption Near Edge Structure) spectroscopy of C K-edge was collected in total electron yield (TEY) mode at the beamline BL12B in the national synchrotron radiation laboratory (NSRL).

2.2 Electrochemical measurements

The working electrodes were containing Co_2P/RGO (or Co_2P), acetylene black and poly (vinyl difluoride) (PVDF) (70:20:10 wt/wt/wt) with N-methyl-2-pyrrolidone (NMP) solvent to form slurry. Then it was casted on copper (Cu) foil and dried at 100 °C for 12 h. The cells (CR2016) were assembled in argon glove box, 1M $LiPF_6$ (ethylene carbonate/dimethyl carbonate with a 1:1 volume ratio) as the electrolyte, metallic lithium and Celgard 2400 as counter electrode and separator, respectively. The electrochemical tests was recorded on a battery test system (Land CT 2001A) between 0.01 and 3.0 V. Electrochemical impedance spectroscopy (EIS) and Cyclic voltammetry (CV) curves were tested on the VSP electrochemical workstation (Bio-logic, France).

3. Results and discussion

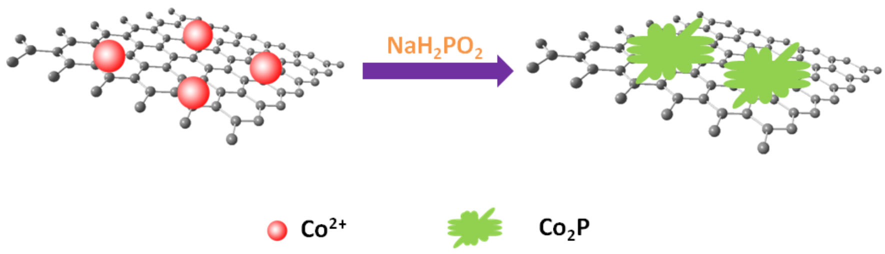

Scheme 1. Schematic illustration for the synthesis of Co_2P/RGO sample.

The schematic illustration for the synthesis of Co_2P/RGO hybrid composite is shown in Scheme 1. In briefly, the Co^{2+} ions were adsorbed on the surface of GO through the electrostatic force, and then mixing with NaH_2PO_2. A low temperature phosphidation procedure was introduced to convert above mixture into Co_2P/RGO.

Fig. 1a shows the XRD patterns of as-prepared bare Co_2P and Co_2P/RGO, which is corresponding to standard orthorhomic structure of Co_2P (JCPDS Card. No. 32-0306). The results are consistent with the previous reports, indicating that both bare Co_2P and Co_2P/RGO composites are successfully synthesized without other impurities by a simple solid reaction.[30,36] The characteristic peak of GO diappears, indicating that GO has been adequately reduced after high temperature calcination.[17] The morphologies and microstructure are shown in Fig. 1(b-f). Obviously, the Co_2P micron spheres are grown on the graphene sheets. The SEM images of Co_2P without graphene are shown in Figure S1, which present the similar morphology with Co_2P/RGO. The TEM image of Co_2P/RGO reveals that flower-like spheres with an average size of 0.5-1.0 um, which are assembled by nanorods, distrbute on the graphene uniformly (Fig. 1c). The HRTEM image presents the Co_2P particles are tightly grown on RGO layer (Fig. 1d). Moreover, the lattice spacing of 0.28 nm can be indexed to the (120) plane indicating good crystallization. EDX elemental mapping images of Co, P and C for a single Co_2P nanorod on RGO further demonstrating that the Co_2P nanoparticles encapsulated by RGO and elements are homogeneously distributed (Fig. 2f).

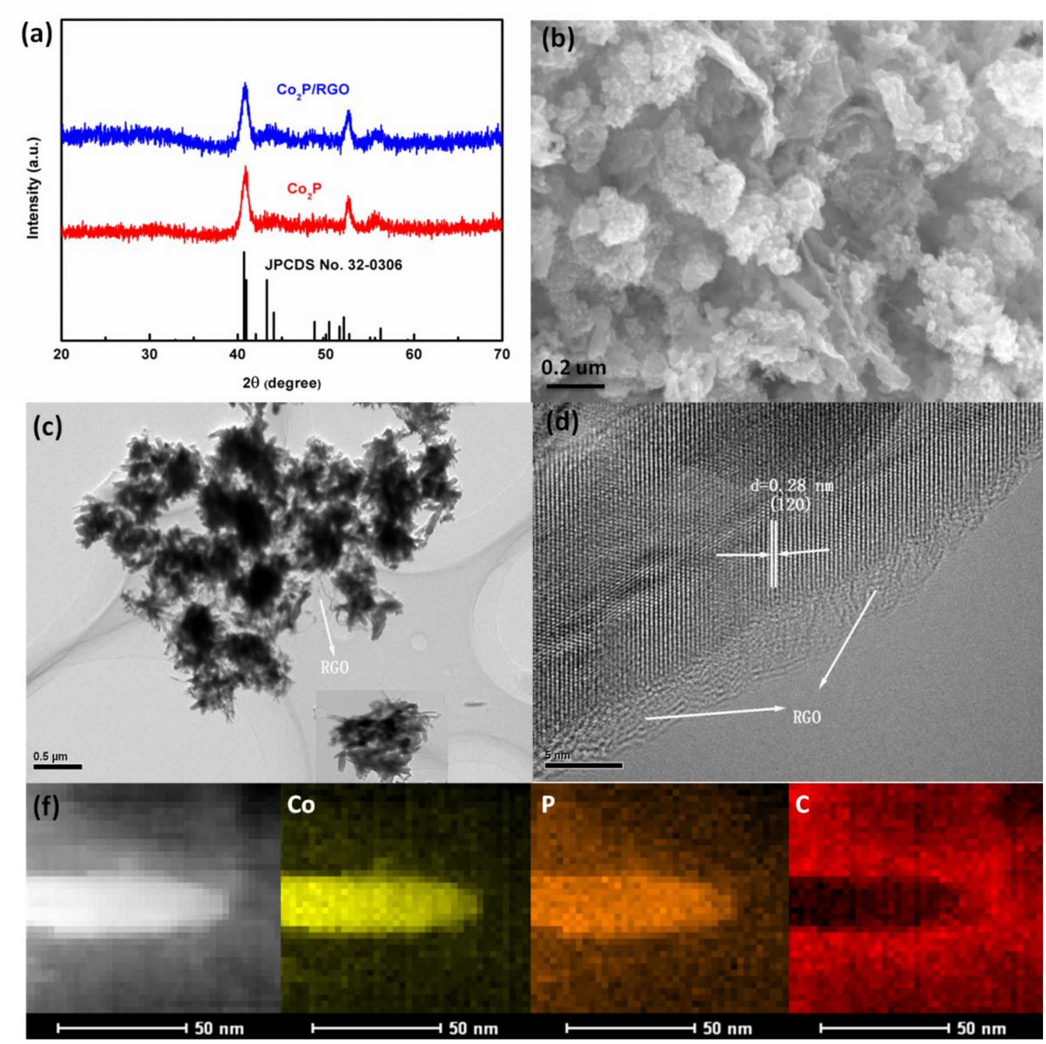

Fig. 1 (a) XRD patterns for Co_2P and Co_2P/RGO samples. (b) SEM image for Co_2P/RGO. (c) and (d) TEM images of Co_2P/RGO. (f) TEM elemental mapping for Co_2P/RGO.

Raman spectroscopy was used to confirm the existence of RGO (See Figure S2). There are two characteristic peaks located at 1349 cm^{-1} (D-band) and 1592 cm^{-1} (G-band). Compare to GO, the higher I_D/I_G ratio in the Co_2P/RGO suggesting that the Co_2P nanorods distributed on the RGO layers and induce more disorder [37,38]. The carbon content in the hybrid composite is determined by TGA curve (Figure S3). The weight loss from 400 °C to 600 °C is about 11.7 % can be attributed to RGO.

To further study the effect of RGO on Co_2P electrode, the XANES (X-ray Absorption Near Edge Structure) spectroscopy of C K-edge are performed. As shown in Fig. 2a, the feature A1 and A3 can be assigned to the C 1s to graphic states of π^* and σ^* transition, respectively [39]. The A2 is the C-O or C=O oxygenated groups induced sp^3 hybridized states. The π^* intensity for Co_2P/RGO is reduced compared with GO, which suggest more charge transfer from Co_2P to graphene, indicating stronger chemical bonding between Co_2P and graphene [40,41]. The lower intensity of feature A2 demonstrates that GO is almost reduced by the heating condition. Moreover, the surface area of both Co_2P and Co_2P/RGO samples were further tested by Nitrogen adsorption/desorption isotherms (Figure S4). Co_2P presents smaller specific surface area of 11.79 m^2 g^{-1}, while the specific surface area of Co_2P/RGO composite increases to 28.91 m^2 g^{-1}. The larger specific surface area could provide better electrode-electrolyte contact and more Li^+-ions sites [42].

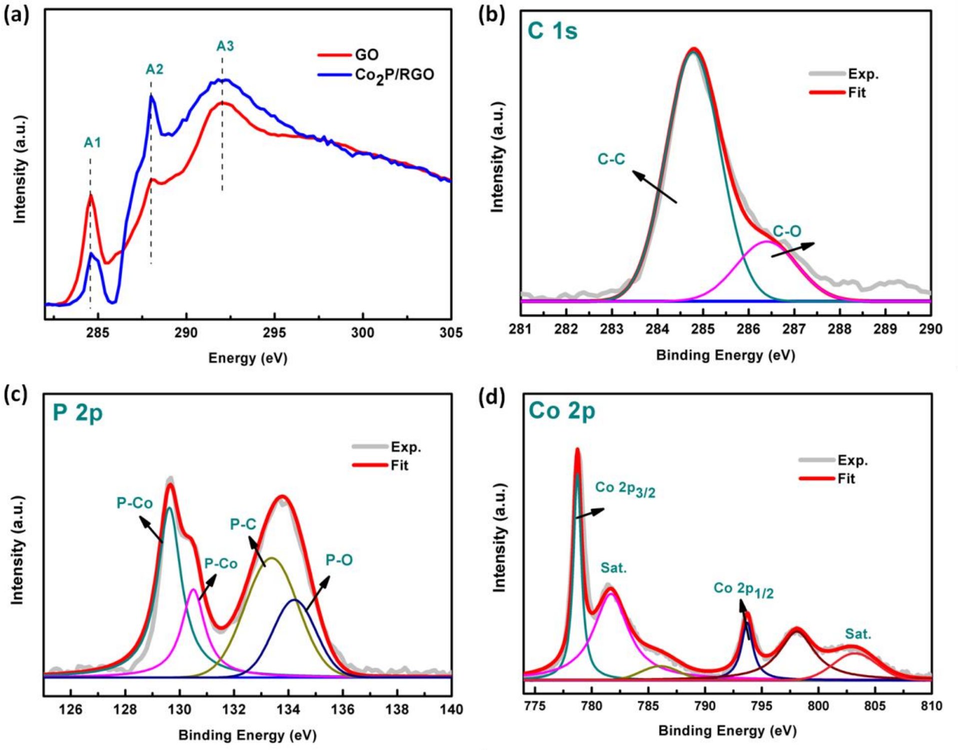

Fig. 2 (a) XANES spectrum for Co_2P/RGO. XPS spectra of C 1s (b), P 2p (c) and Co 2p (d) for Co_2P/RGO.

The chemical state and composition of Co_2P/RGO are measured by XPS. The survey XPS spectrum (Figure S5) demonstrates the existence of Co, P, C and O. The C 1s peak (Fig. 2b) at 284.6 eV and 286.5 eV are corresponding to C-C and C-O species in graphene [43]. It can be seen that the intensities of C-O is much smaller than C-C. This result suggests that GO has been reduced that consistent with the XANES analysis. In the P 2p spectrum (Fig. 2c), two characteristic peak at 129.6 eV and 130.5 eV could be assigned to the P $2p_{3/2}$ and P $2p_{1/2}$ respectively. The Co 2p spectrum has two main peaks located at 778.2 eV (Co $2p_{3/2}$) and 794.1 eV (Co $2p_{1/2}$) with their respective satellite peaks (Fig. 2d). The P $2p_{3/2}$ peak at 129.6 eV and the Co $2p_{3/2}$ peak at 781.2 eV can be ascribed to the binding energies for P 2p and Co 2p in

Co_2P[44,45].

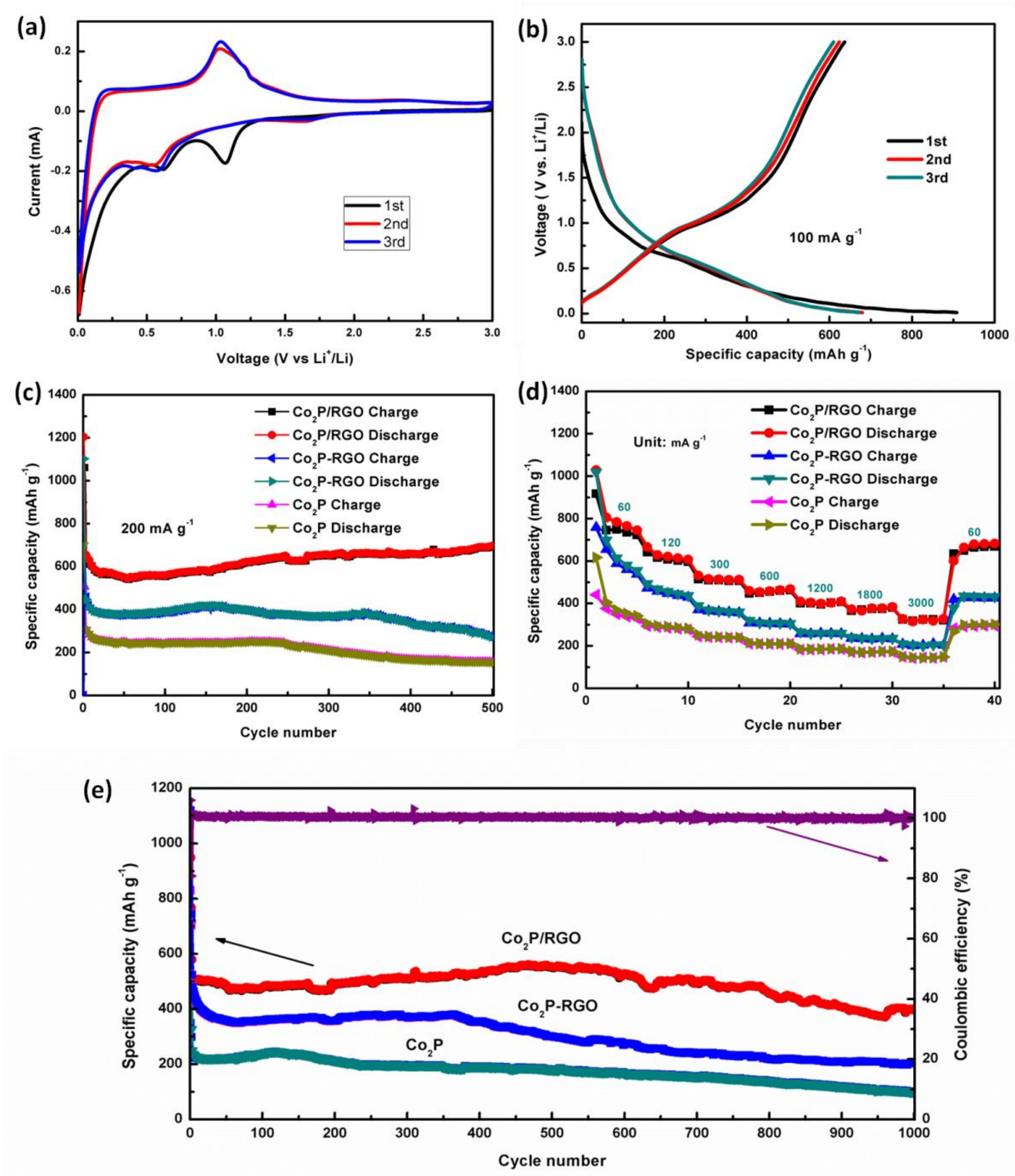

Fig. 3 (a) CV curves of the Co_2P/RGO composite at 0.2 mV s^{-1}. (b) Charge-discharge curves of Co_2P/RGO at 100 mA g^{-1}. (c) Cycling performance of Co_2P/RGO and Co_2P at 200 mA g^{-1}. (d) Rate performance of Co_2P and Co_2P/RGO at various current densities. (e) Cycling performance and coulombic efficiency of Co_2P and Co_2P/RGO at 500 mA g^{-1}.

The lithium storage performance of Co_2P/RGO and Co_2P composites are carried out as anode materials for LIBs. The CV curves of the Co_2P/RGO electrode is shown in Fig. 3a. The peak at around 1.10 V appeared in the first discharge process, which corresponds to the reaction of $Co_2P + 3Li^+ + 3e^- \rightarrow Li_3P + 2Co$ [27]. Another reduction peak at about 0.60 V was attributed to the formation of solid electrolyte interface (SEI) film [33]. The oxidation peak at about 1.0 V can be owning to the decomposition of SEI and Li_3P during charging. After the first cycle, CV curves are nearly over-lapped, suggesting the excellent cyclability. Fig. 3b shows the galvanostatic charge/discharge profiles for the Co_2P/RGO composite at current density of 100 mA g^{-1}. The Co_2P/RGO exhibits discharge and charge capacities are 908 and 637 mAh g^{-1}, respectively, giving a coulmobic efficiency of 70.2 %, which is higher than the previous reports [23,24]. The good overlapping voltage curves indicate the superior reversibility during cycling. The cycling capability of bare Co_2P, Co_2P-RGO and Co_2P/RGO were measured at 200 mA g^{-1}. As shown in Fig.3c, it can be clearly observed that Co_2P/RGO obtained a much higher capacity than the Co_2P-RGO mixture and bare Co_2P. In particularly, a specific capacity of 698 mAh g^{-1} was maintained for Co_2P/RGO after 500 cycles, while the Co_2P-RGO mixture begins to drop after 200 cycles (300 mAh g^{-1}) and bare Co_2P rapidly decayed to 156 mAh g^{-1} at the same condition. Fig. 3d shows the rate capability of bare Co_2P, Co_2P-RGO and Co_2P/RGO. Specially, Co_2P/RGO electrode exhibits higher reversible capacities than that of bare Co_2P and Co_2P-RGO.

The Co_2P/RGO electrode can still exhibit a discharge capacity of around 327 mAh g^{-1} at a current density of 3000 mA g^{-1}. Fig. 3e presents the long cyclability at a current density of 500 mA g^{-1}. The Co_2P/RGO hybrid composite dilivers excellent cyclability, a discharge capacity of about 397 mAh g^{-1} can be maintained even after 1000 cycles with a capacity retention of 77.7 %. In addition, the coulombic efficiency is about 100 %. However, the capacity retention of bare Co_2P and Co_2P-RGO are 57.8% and 43.3 % after 1000 cycles, respectively. The brilliant rate performance and cycle stability of Co_2P/RGO can be attributed to RGO encapsulation, which can not only faciliate Li^+-ions transport and rapid electrons transfer in the composite, but also enhances the structure stability of Co_2P.

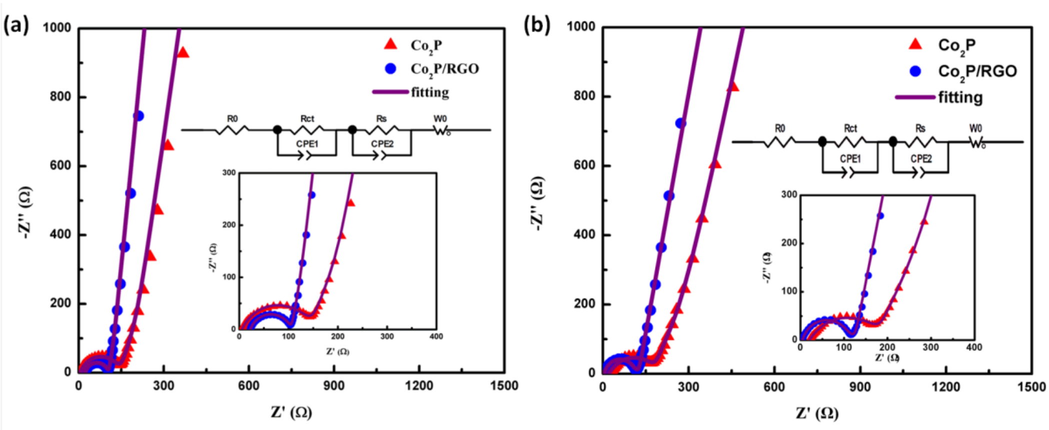

Fig. 4 Nyquist plots of Co_2P and Co_2P/RGO (a) pristine, (b) after 50 cycles.

The Nyquist plots of the Co_2P/RGO and Co_2P samples before and after 50 cycles are shown in Fig. 4, there are semicircles in high frequency and straight lines in the low frequency region. The diameter of semi-circle and the straight line correspond to the charge transfer resistance (R_{ct}) and the Li^+-ions diffusion, respectively [46-50]. The fitting results are summarized in Table S1. Before cycling, the Co_2P/RGO exhibited an R_{ct} of 82.1 Ω, which is lower than that of Co_2P (136.7 Ω), indicating that the Co_2P/RGO has lower charge transfer resistance. Moreover, Co_2P/RGO delivers a higher slope, indicating the faster Li^+-ions diffusion. After cycling, the change of R_{ct} of Co_2P/RGO is almost negligible. While, R_{ct} of Co_2P becomes larger (163.2 Ω) and the change of impedance plot for Co_2P/RGO electrode is much smaller than Co_2P. Hence, the enhancement of the electrochemical properties could be ascribed to the realization of micro/nano structure of Co_2P particles by incorporation of into the graphene network that could eventually lead to fast electrons and Li^+-ions transport.

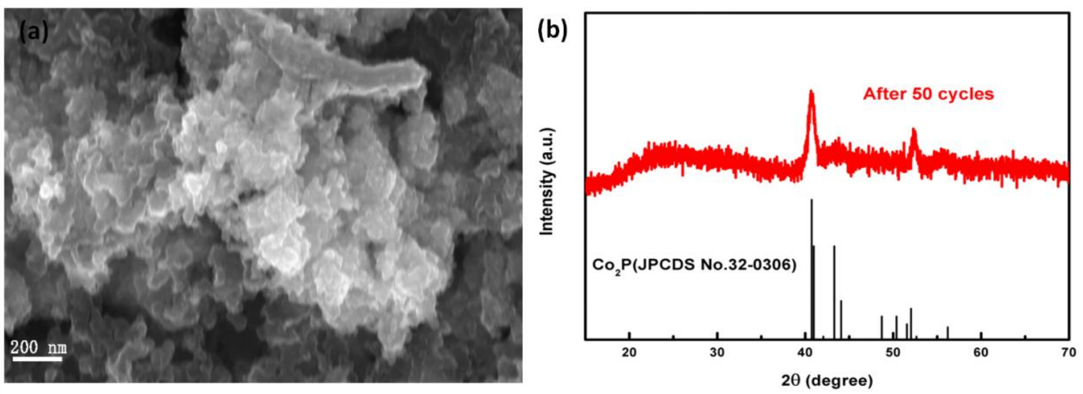

Fig. 5 Co_2P/RGO sample after charging/discharging 50 cycles (a) Ex-situ SEM image, (b) Ex-situ XRD pattern.

To further understand the superior lithium storage performance of the Co_2P/RGO composite, the P 2p XPS spectroscopy after 50 charge/discharge cycles were collected in the Figure. S6. It can be seen that the P-C bond still exists, indicating that the hybrid structure are well maintained during the cycling. Ex-situ SEM and XRD tests were employed after charge/discharge 50 cycles at current density of 200 mA g^{-1}. As shown in Fig. 5, the SEM image shows that morphology and microstructure of hybrid composite was well maintained. Moreover, the XRD pattern is still match with the phase Co_2P. These results further indicate the excellent cyclic capability of the Co_2P/RGO composite.

4. Conclusions

In summary, we developed a facile method to synthesize hierarchically structured Co_2P/RGO hybrid composite and use as anode material for lithium-ion batteries. The Co_2P/RGO hybrid composite exhibited an impressive cyclability of 399 mAh g^{-1} at 500 mA g^{-1} after 1000 cycles and retained a discharge capacity of 327 mAh g^{-1} even at a high current density of 3000 mAh g^{-1}. The unique architecture and graphene modification are responsible for the outstanding electrochemical performance. Such inexpensive synthetic approach and intriguing electrochemical properties of Co_2P/RGO make it as a potential anode material for advanced LIBs.

Acknowledgements

This work is partly supported by the National Natural Science Fo undation of China (No. 11705015, 11605002 and 61604021), Scienc e and Technology Plan Project of Suzhou (No. SYG201738), and Natural Science Foundation of Jiangsu Educational Department (No. 15KJA430001), Six-talent Peak of Jiangsu Province (No. 2012-XCL-036). We sincerely acknowledge the staff of the beamline BL12B in the national synchrotron radiation laboratory (NSRL).

References

[1] S. Chu, A. Majumdar, Opportunities and challenges for a sustainable energy future, Nature 488 (2012) 294-303.

[2] M. Armand, J. M. Tarascon, Building better batteries, Nature 451 (2008) 652−657.

[3] B. Dunn , H. Kamath , J. M. Tarascon, Electrical energy storage for the grid: A battery of choices, Science 334 (2011) 928-935.

[4] G. Chen, L. T. Yan, H. M. Luo, S. J. Guo, Nanoscale engineering of heterstructured anode materials for boosting lithium-ion storage, Adv. Mater. 28 (2017) 7580-7602.

[5] L. W. Ji, Z. Lin, M. Alcoutlabi, X. W. Zhang, Recent developments in nanostructured anode materials for rechargeable lithium-ion batteries, Energy Environ. Sci. 4 (2011) 2682-2699.

[6] Z. Y. Wang, D. Y. Luan, S. Madhavi, C. M. Li, X. W. Lou, α-Fe_2O_3 nanotubes with superior lithium storage capability, Chem. Commun. 47 (2011) 8061-8063.

[7] T. C. Jiang, F. X. Bu, X. X. Feng, I. Shakir, G. L. Hao, Y. X. Xu, Porous Fe_2O_3 nanoframeworks encapsulated within three-demensional graphene as

high-performance flexible anode for lithium-ion battery, ACS nano 5 (2017) 5140-5147.

[8] C. Z. Wang, Y. J. Zhao, D. Z. Su, C. H. Ding, L. Wang, D. Yan, J. B. Li, H. B. Jin, Synthesis of NiO nano octahedron aggregates as high-performance anode materials for lithium ion batteries, Electrochim. Acta 231 (2017) 272-278.

[9] H. R. Du, C. Yuan, K. F. Huang, W. H. Wang, K. Zhang, B. Y. Geng, A novel gelatin-guided mesoporous bowknot-like Co_3O_4 anode material for high-performance lithium-ion batteries, J. Mater. Chem. A 11 (2017) 5342-5350.

[10] W. J. Dong, J. J. Xu, C. Wang, Y. Lu, X. Y. Liu, X. Wang, X. T. Yuan, Z. Wang, T. Q. Lin, M. L. Sui, I. W. Chen, F. Q. Huang, A robust and conductive black Tin oxide nanostructure makes efficient lithium-ion batteries possible, Adv. Mater. DOI: 10.1002/adma.201700136.

[11] X. S. Zhou, L. J. Wan, Y. G. Guo, Binding SnO_2 nanocrystals in nitrogen-doped graphene sheets as anode materials for lithium-ion batteries, Adv. Mater. 25 (2013) 2152-2157.

[12] Q. F. Wang, R. Q. Zou, W. Xia, J. Ma, B. Qiu, A. Mahmood, R. Zhao, Y. Yang, D. G. Xia, Q. Xu, Facile synthesis of ultrasmall CoS_2 nanoparticles within thin N-doped porous carbon shell for high performance lithium-ion batteries, Small 11 (2015) 2511-2517.

[13] G. C. Huang, T. Chen, Z. Wang, K. Chang, W. X. Chen, Synthesis and electrochemical performances of cobalt sulfides/graphene nanocomposite as anode material of Li-ion battery, J. Power Sources 235 (2013) 122-128.

[14] J. R. He, Q. Li, Y. F. Chen, C. Xu, K. R. Zhou, X. Q. Wang, W. L. Zhang, Y. R. Li, Self-assembled cauliflower-like FeS_2 anchored in graphene foam as free-standing anode for high-performance lithium-ion batteries, Carbon 114 (2017) 111-116.

[15] G. X. Pan, F. Cao, X. H. Xia, Y. J. Zhang, Exploring hierarchical FeS_2/C composite nanotubes arrays as advanced cathode for lithium ion batteries, J. Power Sources 332 (2016) 383-388.

[16] B. H. Qu, C. Z. Ma, G. Ji, C. H. Xu, J. Xu, Y. S. Meng, T. H. Wang, J. Y. Lee, Layered SnS_2-reduced graphene oxide composite-a high-capacity, high-rate, and long-cycle life sodium-ion battery anode material, Adv. Mater. 26 (2014) 3854-3859.

[17] Y. Jiang, Y. Z. Feng, B. J. Xi, S. S. Kai, K. Mi, J. K. Feng, J. H. Zhang, S. L. Xiong, Ultrasmall SnS_2 nanoparticles anchored on well-distribued nitrogen-doped graphene sheets for Li-ion and Na-ion batteries, J. Mater. Chem. A 27 (2016) 10719-10726.

[18] T. Xiang, Q. Fang, H. Xie, C. Q. Wu, C. D. Wang, Y. Zhou, D. B. Liu, S. M. Chen, A. Khalil, S. Tao, Q. Liu, L. Song, Vertical 1T-MoS_2 nanosheets with expanded interlayer spacing edged on a graphene frame for high rate lithium-ion batteries, Nanoscale 9 (2017) 6975-6983.

[19] Z. M. Wang, G. Wei, L. Ozawa, Y. L. Cai, Z. X. Cheng, H. Kimura, Nanoporous MoS_2/C composite for high performance lithium ion battery anode material, Electrochim. Acta 239 (2017) 74-83.

[20] P. L. Lou, Z. H. Cui, Z. Q. Jia, J. Y. Sun, Y. B. Tan, X. X. Guo, Monodispersed carbon-coated cubic NiP_2 nanoparticles anchored on carbon nanotubes as ultra-long-life anodes for reversible lithium storage, ACS Nano 11 (2017) 3705-3715.

[21] S. O. Kim, A. Manthiram, Phosphorus-rich CuP_2 embedded in carbon matrix as a high-performance anode for lithium-ion batteries, ACS Appl. Mater. Interfaces 9 (2017) 16221-16227.

[22] F. Han, C. Z. Zhang, J. X. Yang, G. Z. Ma, K. J. He, X. K. Li, Well-dispersed and porous FeP@C nanoplates with stable and ultrafast lithium storage performance through conversion reaction mechamism, J. Mater. Chem. A 4 (2016) 12781-12789.

[23] J. Yang, Y. Zhang, C. C. Sun, H. Z. Liu, L. Q. Li, W. L. Si, W. Huang, Q. Y. Yan, X. C. Dong, Graphene and cobalt phosphide nanowire composite as an anode material for high performance lithium-ion batteries, Nano Res. 9 (2016) 612-621.

[24] Q. S. Xie, D. Q. Zeng, P. Y. Gong, J. Huang, Y. T. Ma, L. S. Wang, D. L. Peng, One-pot fabrication of graphene sheets decorated Co_2P-Co hollow nanospheres for advanced lithium ion battery anodes, Electrochim. Acta 232 (2017) 465-473.

[25] S. L. Liu, H. Z. Zhang, L. Q. Xu, L. B. Ma, X. X. Chen, Solvothermal preparation of tin phosphide as a long-life anode for advanced lithium and sodium ion batteries, J. Power Sources 304 (2016) 346-353.

[26] M. Walter, M. I. Bodnarchuk, K. V. Kravchyk, M. V. Kovalenko, Evalution of metal phosphide nanocrystals as anode materials for Na-ion batteries, Chimia 69 (2015) 724-728.

[27] M. Sun, H. J. Liu, J. H. Qu, J. H. Li, Earth-rich transition metal phosphide for energy conversion and storage, Adv. Energy Mater. 6 (2016) 1600087.

[28] X. He, R. Wang, M. C. Stan, E. Paillard, J. Wang, H. Frielinghaus, J. Li, In situ investigations on the structural and morphological changes of metal phosphides as anode materials in lithium-ion batteries, Adv. Mater. Interfaces 4 (2017) 1601047.

[29] M. H. Chen, W. W Zhou, M. L. Qi, J. H. Yin, X. H. Xia, Q. G. Chen, Exploring highly porous Co_2P nanowire arrays for electrochemical energy storage, J. Power Sources, 342 (2017) 964-969.

[30] X. j. Chen, M. Cheng, D. Chen, R. M. Wang, Shape-controlled synthesis of Co_2P nanostructures and their application in supercapacitors, ACS Appl. Mater. Interfaces 8 (2016) 3892-3900.

[31] S. L. Liu, L. Yan, H. L. Li, Solvothermal synthesis of flower-like Co_2P nanostructures and its electrochemical performance, Sci. Adv. Mater. 6 (2014) 746-750.

[32] D. Yang, J. X. Zhu, X. H. Rui, H. T. Tan, R. Cai, H. E. Hoster, D. T. W. Yu, H. H. Hng, Q. Y. Yan, Synthesis of cobalt phosphides and their application as anodes for lithium ion batteries, ACS Appl. Mater. Interfaces 5(2013) 1093-1099.

[33] A. L. Lu, X. Q. Zhang, Y. Z. Chen, Q. S. Xie, Q. Q. Qi, Y. T. Ma, D. L. Peng, Synthesis of Co_2P/graphene nanocompsoites and their enhanced properties as anode materials for lithium ion batteries, J. Power Sources 295 (2015) 329-335.

[34] Y. Zhao, L. P. Wang, M. T. Sougrati, Z. X. Feng, Y. Leconte, A. Fisher, ,. Srinivasan, Z. Xu, A review on design strategies for carbon based metal oxides and sulfides nanocomposites for high performance Li and Na battery anodes, Adv. Energy Mater. 7 (2017) 1601424.

[35] C. Wu, Y.J. Yang, D. Dong, Y. H. Zhang, J. H. Li, In situ coupling of CoP polyhedrons and carbon nanotubes as highly efficient hydrogen evolution reaction electrocatalyst, Small, 13 (2017) 1602873.

[36] M. Cheng, H. Fan, Y. Xu, R. Wang, X. Zhang, Hollow Co_2P nanoflowers assembled from nanorods for ultralong cycle-life supercapacitors, Nanoscale, 9 (2017) 14162-14171.

[37] D. C. Marcano, D. V. Kosynkin, J. M. Berlin, A. Sinitskii, Z. Sun, A. Slesarev, L. B. Alemany, W. Lu, J. M. Tour, Improved synthesis of graphene oxide, ACS nano 2010, 4 4806–4814.

[38] S. Tao, W. F. Huang, G. X. Wu, X. B. Zhu, X. B. Wang, M. Zhang, S. H. Wang, W. S. Chu, L. Song, Z. Y. Wu. Performance enhancement of lithium-ion battery with $LiFePO_4$@C/RGO hybrid electrode. Electrochimi. Acta 2014; 144: 406-411.

[39] S. J. Patil, J. H. Kim, D. W. Lee, Graphene-nanosheet wrapped cobalt sulphide as a binder free hybrid electrode for asymmetric solid-state supercapacitor, 342 (2017) 652-665.

[40] J. Zhong, J. J. Deng, B. H. Mao, T. Xie, X. H. Sun, Z. G. Mou, C. H. Hong, P. Yang, S. D. Wang. Probing solid state N-Doping in graphene by X-ray absorption near-edge structure spectroscopy. Carbon 2012; 50: 321-41.

[41] R. P. Gandhiraman, D. Nordlind, C. Jassica, J. E. Koehne, B. Chen, M. Meyyappan. X-ray absorption study of graphene oxide and transition metal oxide nanocomposites. J. Phys. Chem. C 2014; 118: 18706-12.

[42] C. H. Chuang, T. F. Wang, Y. C. Shao, Y. C. Yeh, D. Y. Wang, C. W. Chen, J. W. Chiou, S. C. Ray, W. F. Pong, L. Zhang, J. F. Zhu. The effect of thermal reduction on the photoluminescence and electronic structure of graphene oxides. Sci. Rep. 2014; 4: 4525.

[43] X. M. Zhu, X. Y. Jiang, X. Chen, X. L. Liu, L. F. Xiao, Y. L. Cao, Fe_2O_3 amorphous nanoparticles/graphene composite as high-performance anode materials for lithium-ion batteries, J. Alloys and Compd. 711 (2017) 15-21.

[44] D. Das, A. Das, M. Reghunath, K. K. Nanda, Phosphine-free avenue to Co_2P nanoparticle encapsulated N, P Co-doped CNTs: a novel non-enzymatic glucose sensor and an efficient electrocatalyst for oxygen evolution reaction, Green Chem. 19 (2017) 1327-1335.

[45] Z. Y. Jin, P. P. Li, D. Xiao, Metallic Co_2P ultrathin nanowires distinguished from CoP as robust electrocatalysts for overall water-splitting, Green Chem. 18 (2016) 1459-1464.

[46] M. H. Zhuang, X. W. Ou, Y. B. Dou, L. L. Zhang, Q. C. Zhang, R. Z. Wu, Y. Ding, M. H. Shao, Z. T. Luo, Polymer-embedded fabrication of Co_2P

nanoparticles encapsulated in N, P-doped graphene for hydrogen generation, Nano Lett. 16 (2016) 4691-4698.

[47] J. M. Wang, W. R. Yang, J. Q. Liu, CoP_2 nanoparticles on reduced graphene oxide sheets as super-efficient bifunctional electrocatalyst for full water splitting, J. Mater. Chem. A 4 (2016) 4686-4690.

[48] Y. Y. Feng, H. J. Zhang, Y. P. Mu, W. X. Li, J. L. Sun, K. Wu, Y. Wang, Monodisperse sandwich-like coupled quasi-graphene sheets encapsulating Ni_2P nanoparticles for enhanced lithium-ion batteries, Chem. Eur. J. 21 (2015) 9229-9235.

[49] X. Y. Zhou, S. M. Chen, J. Yang, T. Bai, Y. P. Ren, H. Y. Tian, Metal-organic frameworks derived okra-like SnO_2 encapsulated in nitrogen-doped graphene for lithium ion battery, ACS Appl. Mater. Interfaces 9 (2017) 14309-14318.

[50] J. Xie, S. Y. Liu, G. S. Cao, T. J. Zhu, X. B. Zhao, Self-assemblely of CoS_2/graphene nanoarchitecture by a facile one-pot route and its improved electrochemical Li-Storage properties, Nano Energy 2 (2013) 49-56.